

# A Skeletal Measure of 2D Shape Similarity

Andrea Torsello and Edwin R. Hancock

Dept. of Computer Science, University of York  
Heslington, York, YO10 5DD, UK  
atorsell@cs.york.ac.uk

**Abstract.** This paper presents a geometric measure that can be used to gauge the similarity of 2D shapes by comparing their skeletons. The measure is defined to be the rate of change of boundary length with distance along the skeleton. We demonstrate that this measure varies continuously when the shape undergoes deformations. Moreover, we show that ligatures are associated with low values of the shape-measure. The measure provides a natural way of overcoming a number of problems associated with the structural representation of skeletons. The first of these is that it allows us to distinguish between perceptually distinct shapes whose skeletons are ambiguous. Second, it allows us to distinguish between the main skeletal structure and its ligatures, which may be the result of local shape irregularities or noise.

## 1 Introduction

The skeletal abstraction of 2D and 3D objects has proved to be an alluring yet highly elusive goal for over 30 years in shape analysis. The topic is not only important in image analysis, where it has stimulated a number of important developments including the medial axis transform and iterative morphological thinning operators, but is also an important field of investigation in differential geometry and biometrics where it has led to the study of the so-called Blum skeleton [4]. Because of this, the quest for reliable and efficient ways of computing skeletal shape descriptors has been a topic of sustained activity. Recently, there has been a renewed research interest in the topic which has been aimed at deriving a richer description of the differential structure of the object boundary. This literature has focused on the so-called shock-structure of the reaction-diffusion equation for object boundaries.

The idea of characterising boundary shape using the differential singularities of the reaction equation was first introduced into the computer vision literature by Kimia Tannenbaum and Zucker [9]. The idea is to evolve the boundary of an object to a canonical skeletal form using the reaction-diffusion equation. The skeleton represents the singularities in the curve evolution, where inward moving boundaries collide. The reaction component of the boundary motion corresponds to morphological erosion of the boundary, while the diffusion component introduces curvature dependent boundary smoothing. In practice, the skeleton can be computed in a number of ways [1,11]. Recently, Siddiqi, Tannenbaum and Zucker have shown how the eikonal equation which underpins the

reaction-diffusion analysis can be solved using the Hamilton-Jacobi formalism of classical mechanics [6,17].

One of the criticisms that can be levelled at existing skeletonisation methods is their sensitivity to small boundary deformations or ligatures. Although these can be reduced via curvature dependent smoothing, they may have a significant effect on the topology of the extracted skeleton.

Once the skeletal representation is to hand then shapes may be matched by comparing their skeletons. Most of the work reported in the literature adopts a structural approach to the matching problem. For instance, Pelillo, Siddiqi and Zucker use a sub-tree matching method [14]. This method is potentially vulnerable to structural variations or errors due to local deformations, ligature instabilities or other boundary noise. Tithapura, Kimia and Klein have a potentially more robust method which matches by minimising graph-edit distance [10,20].

One of the criticisms of these structural matching methods is that perceptually distinct shapes may have topologically identical skeletons which can not be distinguished from one-another. Moreover, small boundary deformations may significantly distort the topology of the skeleton.

We draw two observations from this review of the related literature. The first is that the existing methods for matching are based on largely structural representations of the skeleton. As a result, shapes which are perceptually different but which give rise to the same skeleton topology are ambiguous with one-another. For this reason we would like to develop a metrical representation which can be used to assess the differences in shape for objects which have topologically identical skeletons. Secondly, we would also like to be able to make comparisons between shapes that are perceptually close, but whose skeletons exhibit topological differences due to small but critical local shape deformations.

To meet these dual goals, our shape-measure must have three properties. First, it must be continuous over local regions in shape-space in which there are no topological transitions. If this is the case then it can be used to differentiate shapes with topologically identical skeletons. Secondly, it must vary smoothly across topological transitions. This is perhaps the most important property since it allows us to define distances across transitions in skeleton topology. In other words, we can traverse the skeleton without encountering singularities. Thirdly, it must distinguish between the principal component of the skeleton and its ligatures [2]. This will allow us to suppress instabilities due to local shape deformations.

Commencing from these observations, we opt to use a shape-measure based on the rate of change of boundary length with distance along the skeleton. To compute the measure we construct the osculating circle to the two nearest boundary points at each location on the skeleton. The rate of change of boundary length with distance along the skeleton is computed by taking neighbouring points on the skeleton. The corresponding change in boundary length is computed by determining distance along the boundary between the corresponding points of con-

tact for the two osculating circles. The boundary distances are averaged for the boundary segments either side of the skeleton.

This measurement has previously been used in the literature to express *relevance* of a branch when extracting or pruning the skeleton [11,12]. We show that rate of change of boundary length with distance along the skeleton has a number of interesting properties. The consequence of these properties is that the descriptive content of the measure extend beyond simple feature saliency, and can be used to attribute the relational structure of the skeleton to achieve a richer description of shape. Furthermore, we demonstrate that there is an intimate relationship between the shape measure and the divergence of the distance map. This is an important observation since the divergence plays a central role when the skeleton is computed using the Hamilton-Jacobi formalism to solve the eikonal equation.

## 2 Skeleton Detection

A great number of papers have been written on the subject of skeleton detection. The problem is a tricky one because it is based on the detection of singularities on the evolution of the eikonal equation on the boundary of the shape.

The eikonal equation is a partial differential equation that governs the motion of a wave-front through a medium. In the case of a uniform medium the equation is  $\frac{\partial}{\partial t} C(t) = \alpha N(t)$ , where  $C(t) : [0, s] \rightarrow \mathbb{R}^2$  is the equation of the front at time  $t$  and  $N(t) : [0, s] \rightarrow \mathbb{R}^2$  is the equation of the normal to the wave front in the direction of motion and  $\alpha$  is the propagation speed. As the wave front evolves, opposing segments of the wave-front collide, generating a singularity. This singularity is called a shock and the set of all such shocks is the skeleton of the boundary defined by the original curve. This realisation of the eikonal equation is also referred to as the reaction equation.

To detect the singularities in the eikonal equation we use the Hamilton-Jacobi approach presented by Siddiqi, Tannenbaum, and Zucker [6,17]. Here we review this approach.

We commence by defining a distance-map that assigns to each point on the interior of an object the closest distance  $D$  from the point to the boundary (i.e. the distance to the closest point on the object boundary). The gradient of this distance-map defines a field  $F$  whose domain is the interior of the shape. The field is defined to be  $F = \nabla D$ , where  $\nabla = (\frac{\partial}{\partial x}, \frac{\partial}{\partial y})^T$  is the gradient operator. The trajectory followed by each boundary point under the eikonal equation can be described by the ordinary differential equation  $\dot{x} = F(x)$ , where  $x$  is the coordinate vector of the point. This is a Hamiltonian system, i.e. wherever the trajectory is defined the divergence of the field is zero [13]. However, the total inward flux through the whole shape is non zero. In fact, the flux is proportional to the length of the boundary.

The divergence theorem states that the integral of the divergence of a vector-field over an area is equal to the flux of the vector field over the enclosing boundary of that area. In our case,  $\int_A \nabla \cdot F d\sigma = \int_L F \cdot n dl = \Phi_A(F)$ , where  $A$

is any area,  $F$  is a field defined in  $A$ ,  $d\sigma$  is the area differential in  $A$ ,  $dl$  is the length differential on the border  $L$  of  $A$ , and  $\Phi_A(F)$  is the outward flux of  $F$  through the border  $L$ .

By virtue of the divergence theorem we have that, within the interior, there are points where the system is not conservative. The non-conservative points are those where the boundary trajectory is not well defined, i.e. where there are singularities in the evolution of the boundary. These points are the so-called shocks or skeleton of the shape-boundary. Shocks are thus characterised by locations where  $\nabla \cdot F < 0$ . Unfortunately, skeletal points are, also, ridges of the distance map  $D$ , that is  $F = \nabla D$  is not uniquely defined in those points, but have different values on opposite sides of the watershed. This means that the calculation the derivatives of  $F$  gives raise to numerical instabilities. To avoid this problem we can use the divergence theorem again. We approximate the divergence with the outward flux through a small area surrounding the point. That is  $\nabla \cdot F(x) \approx \Phi_U(F)(x)$ , where  $U$  is a *small* area containing  $x$ . Thus, calculating the flux through the immediate neighbors of each pixel we obtain a suitable approximation of  $\nabla \cdot F(x)$ .

### 2.1 Locating the Skeleton

The thinning of the points enclosed within the boundary to extract the skeleton is an iterative process which involves eliminating points with low inward flux. The steps in the thinning and localisation of the skeleton are as follows

- At each iteration of the thinning process we have a set of points that are candidates for elimination. We remove from this set the point with the lowest inward flux.
- Next we check whether the point is topologically simple, i.e. whether it can be eliminated without splitting the remaining point-set.
- If the point is not simple, then it must be part of the skeleton. Thus we retain it.
- If the point is simple, then we check whether it is an endpoint. If the point is simple and not an endpoint, then we eliminate it from the image. If this is the case then we add to the candidate set the points in its 8-neighborhood that are still part of the thinned shape (i.e. points that were not previously eliminated).
- If a simple point is also an endpoint, then the decision of whether or not it will be eliminated is based on the inward flux value. If the flux value is below a certain threshold we eliminate the point in the manner described above. Otherwise we retain the point as part of the skeleton.

We initialise this iterative process by placing every boundary point in the candidate set. We iterate the process until we have no more candidates for removal. The residual points will all belong to the skeleton.

### 3 The Shape-Measure and Its Properties

When the skeleton is computed in this way, then the eikonal equation induces a map from a point in the skeleton to a set of points on the boundary of the shape. That is, there is a correspondence between a point on the skeleton and the set of points on the boundary whose trajectories intercept it under the motion induced by the eikonal equation. The cardinality of this set of corresponding points on the boundary can be used to classify the local topology of the skeleton in the following manner

- the cardinality is greater than or equal to 3 for junctions.
- for endpoints the cardinality is number from 1 to a continuum.
- for the general case of points on branches of the skeleton, the cardinality is exactly 2.

As a result of this final property, any segment of a skeleton branch  $s$  is in correspondence with two boundary segments  $l_1$  and  $l_2$ . This allows us to assign to a portion of the skeleton the portion of the boundary from which it arose. For each internal point in a skeleton branch, we can thus define the local ratio between the length of the generating boundary segment and the length of the generated skeleton segment. The rate of change of boundary length with skeleton length is defined to be  $dl/ds = dl_1/ds + dl_2/ds$ . This ratio is our measure of the relevance of a skeleton segment in the representation of the 2D shape-boundary.

Our proposal in this paper is to use this ratio as a measure of the local relevance of the skeleton to the boundary-shape description. In particular we are interested in using the measure to identify ligatures [2]. Ligatures are skeleton segments that link the logically separate components of a shape. They are characterised by a high negative curvature on the generating boundary segment. The observation which motivates this proposal is that we can identify ligature by attaching to each infinitesimal segment of skeleton the length of the boundary that generated it. Under the eikonal equation, a boundary segment with high negative curvature produces a rarefaction front. This front will cause small segments to grow in length throughout their evolution, until they collide with another front and give rise to a so-called shock. This means that very short boundary segments generate very long skeleton branches. Consequently, when a skeleton branch is a ligature, then there is an associated decrease in the boundary-length to shock-length ratio. As a result our proposed skeletal shape measure 'weights' ligature less than other points in the same skeleton branch.

To better understand the rate of decrease of the boundary length with skeletal length, we investigate its relationship to the local geometry of the osculating

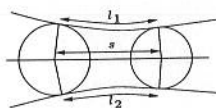


Fig. 1. Geometric quantities

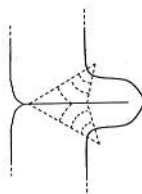


Fig. 2. Ligature points are generated by short boundary segments

circle to the object boundary. We have

$$dl_1/ds = \frac{\cos \theta}{1 - rk_1} \quad \text{and, similarly,} \quad dl_2/ds = \frac{\cos \theta}{1 - rk_2} \quad (1)$$

where  $r$  is the radius of the osculating circle,  $k_i$  is the curvature of the mapped segment on the boundary, oriented so that positive curvatures imply the osculating circle is in the interior of the shape, and, finally,  $\theta$  is the angle between the tangent to the skeleton and the tangent to the corresponding point on the boundary. These formulae show that the metric is inversely proportional to negative curvature and radius. That is, if we fix a negative curvature  $k_1$ , the measure decreases as the skeleton gets further away from the border. Furthermore, the measure decreases faster when the curvature becomes more negative.

Another important property of the shape-measure is that its value varies smoothly across shape deformations, even when these deformations impose topological transitions to the skeleton. To demonstrate this property we make use of the taxonomy of topological transition of the skeleton compiled by Giblin and Kimia [7]. According to this taxonomy, a smooth deformation of the shape induces only two types of transition on the skeleton (plus their time reversals). The transitions are *branch contraction* and *branch splicing*. A deformation *contracts* a branch joining two junctions when it moves the junctions together. Conversely, it *splices* a branch when it reduces in size, smoothes out, or otherwise eliminates the protrusion or sub-part of a shape that generates the branch.

A deformation that contracts or splices a skeleton branch, causes the global value of the shape-measure along the branch to go to zero as the deformation approaches the topological transition. This means that a decreasing length of boundary generates the branch, until the branch disappears altogether.

When a deformation causes a contraction transition, both the length of the skeleton branch and the length of the boundary segments that generate the branch go to zero. A more elusive case is that of splicing. Through a splicing deformation, a decreasing length of boundary maps to the skeleton branch. This is because either the skeleton length and its associated boundary length are both reduced, or because the deformation allows boundary points to be mapped to adjacent skeleton branches. For this reduction in the length of the generating boundary, we do not have a corresponding reduction of the length of the skeleton branch. In fact, in a splice operation the length of the skeleton branch is a lower bound imposed by the presence of the ligature. This is the major cause of the perceived instability of the skeletal representation. Weighting each point on the boundary which gave rise to a particular skeleton branch allows us to eliminate the contributions from ligatures, thus smoothing the instability. Since a smooth shape deformation induces a smooth change in the boundary, the total shape-measure along the branch has to vary smoothly through any deformation.

Just like the radius of the osculating circle, key shape elements such as necks and seeds are associated with local variations of the length ratio. For instance, a neck is a point of high rarefaction and, thus, a minimum of the shape-measure along the branch. A seed is a point where the front of the evolution of the eikonal equation concentrates, and so is characterised by a maximum of the ratio.

Another important property of the shape-measure is its invariance to bending of the shape. Bending invariance derives from the fact that, if we bend the shape, we lose from one side the same amount of boundary-length that we gain on the opposite side. To see this we let  $k$  be the curvature on the skeleton, and  $k_1$  and  $k_2$  be the inward curvature on the corresponding boundary points. Further, suppose that  $\theta$  is the angle between the border tangent and the skeleton tangent.

Let  $p = 2k + \frac{k_1 \cos \theta}{1-rk_1} = \frac{k_2 \cos \theta}{1-rk_2}$ , thus we have  $p = k_2(\cos \theta + pr)$  and

$$k_2 = \frac{p}{\cos \theta + pr} = \frac{2k + \frac{\cos \theta}{1-rk_1} k_1}{\cos \theta + 2rk + \frac{r \cos \theta}{1-rk_1} k_1} = \frac{2k(1-rk_1) + k_1 \cos \theta}{2rk(1-rk_1) + \cos \theta}$$

Substituting the above in (1), we have

$$dl_2/ds = \frac{\cos \theta}{1 - r \frac{2k(1-rk_1) + k_1 \cos \theta}{2rk(1-rk_1) + \cos \theta}} = \frac{2rk(1-rk_1) + \cos \theta}{1-rk_1}$$

Thus we find that  $dl_2/ds = 2rk + dl_1/ds$ , or  $dl_2/ds - rk = dl_1/ds + rk$ . That is, if we bend the image enough to cause a curvature  $k$  in the skeleton, what we lose on one side we get back on the other.

### 4 Measure Extraction

The extraction of the skeletal shape measure is a natural by-product which comes for free when we use the Hamilton-Jacobi approach for skeleton extraction. This is a very important property of this shape-measure. Using the divergence theorem we can transport a quantity linked to a potentially distant border to a quantity local to the skeleton. Using this property, we can prove that the border length to shock length ratio is proportional to the divergence of the gradient of the distance map.

As we have already mentioned, the eikonal equation induces a system that is conservative everywhere except on the skeleton. That is, given the field  $F$  defined as the gradient of the distance map, the divergence of  $F$  is everywhere zero, except on the skeleton.

To show how the shape-measure can be computed in the Hamilton-Jacobi setting, we consider a skeleton segment  $s$  and its  $\epsilon$ -envelope. The segment  $s$  maps to two segment borders  $l_1$  and  $l_2$ . The evolution of the points in these border segments define two areas  $A_1^\epsilon$  and  $A_2^\epsilon$  enclosed within the  $\epsilon$ -envelope of  $s$ , the segments of boundary  $l_1$  and  $l_2$ , and the trajectories  $b_1^1$  and  $b_1^2$ , and  $b_2^1$  and  $b_2^2$  of the endpoints of  $l_1$  and  $l_2$ . The geometry of these areas is illustrated in figure 3.

Since  $\nabla \cdot F = 0$  everywhere in  $A_1^\epsilon$  and  $A_2^\epsilon$ , by virtue of the divergence theorem we can state that the flux from the two areas are both zero, i.e.  $\Phi_{A_1^\epsilon}(F) = 0$  and  $\Phi_{A_2^\epsilon}(F) = 0$ . The trajectories of the endpoints of the border are, by construction, parallel to the field, so the normal is everywhere normal to the field and thus there is no flux through the segments  $b_1^1$ ,  $b_1^2$ ,  $b_2^1$  and  $b_2^2$ . On the other hand the

field on the shape-boundary is always normal to the boundary. Hence, the flux through the border segments  $l_1$  and  $l_2$  is equal to the length  $\ell(l_1)$  and  $\ell(l_2)$  of the segments  $l_1$  and  $l_2$  respectively.

Since  $\Phi_{A_1^\epsilon}(F) = 0$  and  $\Phi_{A_2^\epsilon}(F) = 0$  the flux that enters through the border segments  $l_1$  and  $l_2$  has to exit through the  $\epsilon$ -envelope of  $s$ . That is, if  $\epsilon_1$  and  $\epsilon_2$  are the sides of  $A_1^\epsilon$  and  $A_2^\epsilon$  on the  $\epsilon$ -envelope of  $s$ , we have  $\Phi_{\epsilon_1}(F) = \Phi_{l_1}(F)$  and  $\Phi_{\epsilon_2}(F) = \Phi_{l_2}(F)$ . This, in turn, implies that the flux through the whole  $\epsilon$ -envelope of  $s$  is  $\Phi_\epsilon(F) = \ell(l_1) + \ell(l_2)$ .

Since  $\lim_{\epsilon \rightarrow 0} \int_\epsilon \nabla \cdot F d\epsilon = \int_s \nabla \cdot F ds$ , and the value of the flux through the  $\epsilon$ -envelope of  $s$  is independent of  $\epsilon$ , we have  $\int_s \nabla \cdot F ds = \ell(l_1) + \ell(l_2)$ .

Taking the first derivative with respect to  $ds$  we have, for each non-singular point in the skeleton,  $\nabla \cdot F = dl_1/ds + dl_2/ds$ .

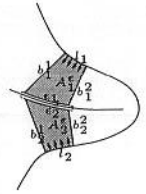


Fig. 3. The flux through the border and through  $\epsilon$  are equal

### 4.1 Computing the Distance between Skeletons

This result allows us to calculate a global shape-measure for each skeleton branch during the branch extraction process. For our matching experiments we have used a simple graph representation where the nodes are junctions or endpoints, and the edges are branches of the skeleton. When we have completed the thinning of the shape boundary and we are left only with the skeleton, we pick an endpoint and start summing the values of the length ratio for each skeleton points until we reach a junction. This sum  $\sum_{i \in s} \nabla \cdot F(x_i)$  over every pixel  $x_i$  of our extracted skeleton branch is an approximation of  $\int_s \nabla \cdot F ds = \int_s (dl_1/ds + dl_2/ds) = \ell(l_1) + \ell(l_2)$  the length of the border that generates the skeleton branch.

At this point we have identified a branch and we have calculated the total value of the length-ratio along that branch, or, in other words, we have computed the total length of the border that generated the branch. We continue this process until we have spanned each branch in the entire skeleton. Thus we obtain a weighted graph representation of the skeleton. In the case of a simple shape, i.e. a shape with no holes, the graph has no cycles and thus is an (unrooted) tree.

Given this representation we can cast the problem of computing distances between different shapes as that of finding the tree edit distance between the weighted graphs for their skeletons.

*Tree edit distance* is a generalization to trees of *String edit distance*. The edit distance is based on the existence of a set  $S$  of basic edit operation on a tree and a set  $C$  of costs, where  $c_s \in C$  is the cost of performing the edit operation  $s \in S$ . The choice of the basic edit operations, as well as their cost, can be tailored to the problem, but common operations include leaf pruning, path merging, and, in case of an attributed tree, change of attribute. Given two trees  $T_1$  and  $T_2$ , the set  $S$  of basic edit operations, and the cost of such operation  $C = c_s, s \in S$ , we call an *edit path* from  $T_1$  to  $T_2$  a sequence  $s_1, \dots, s_n$  of basic edit operations that transform  $T_1$  into  $T_2$ . The length of such path is  $l = c_{s_1} + \dots + c_{s_n}$ ; the *minimum*

length edit path from  $T_1$  to  $T_2$  is the path from  $T_1$  to  $T_2$  with minimum length. The length of the minimum length path is the tree edit distance.

With our measure assigned to each edge of the tree, we define the cost of matching two edges as the difference of the total length ratio measure along the branches. The cost of eliminating an edge is equivalent to the cost of matching it to an edge with zero weight, i.e. one along which the total length ratio is zero.

### 5 Experimental Results

In this section we assess the ability of the proposed measure to discriminate between different shapes that give rise to skeletons with the same topology. We will also assess how smoothly the overall measure goes through transitions.

As demonstrated earlier in the paper, we know that the length ratio measure should be stable to any local shape deformation, including those that exhibit an instability in shock length. This kind of behaviour at local deformations is what has led to the idea that the skeleton is an unstable representation of shape.

To demonstrate the stability of the skeletal representation when augmented with the length ratio measurement, we have generated a sequence of images of a rectangle with a protrusion on one side (Figure 4). The size of the protrusion is gradually reduced throughout the sequence, until it is completely eliminated in the final image. In figure 5 we plot the global value of the length ratio measure for the shock branch generated by the protrusion. It is clear that the value of the length ratio measure decreases monotonically and quite smoothly until it becomes zero when the protrusion disappears.

In a second set of experiments we have aimed to assess the ability of the length ratio measure to distinguish between structurally similar shapes. To do this we selected two shapes that were perceptually different, but which possessed skeletons with a very similar topology. We, then, generated an image sequence in which the two shapes were morphed into one-another. Here the original shapes are the start and end frames of the sequence. At each frame in the sequence we calculated the distance between the start and end shapes.

We repeated this experiment with two morphing sequences. The first sequence morphed a sand shark into a swordfish, while the second morphed a donkey into a hare.

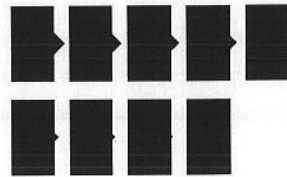


Fig. 4. A “disappearing” protrusion which causes instability in shock-length, but not in our measure

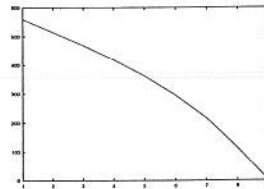


Fig. 5. The measure of the skeleton segment generated by a protrusion



Fig. 6. Morphing sequences and their corresponding skeletons: sand shark to swordfish on the left, and donkey to hare on the right

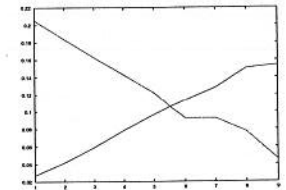
To determine the distance between two shapes we used the Euclidean distance between the normalized weights of matched edges. In other words, the distance is  $D(A, B) = \sqrt{\sum_i (e_i^A - e_i^B)^2}$  where  $e_i^A$  and  $e_i^B$  are the normalised weights on the corresponding edges indexed by  $i$  on the shapes denoted by  $A$  and  $B$ . The normalised weights are computed by dividing the raw weights by the sum of the weights of each tree.

We apply this normalized length ratio measure to ensure scale invariance: two identical shapes scaled to different proportion would have different ratios due to the scale difference, but measure along equivalent branches of the two shapes would vary by a constant scale factor: the ratio of the lengths of the borders. Since the the sum of the weights of the edges of a tree is equal to the total length of the border, dividing the weights in each branch by this quantity we have reduced the two measurements to the same scale. In this way the relevant quantity is not the absolute magnitude for a branch, but the magnitude ratio with other branches.

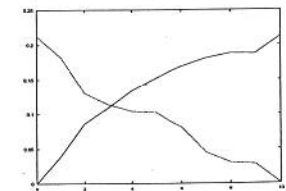
There is clearly an underlying correspondence problem involved in calculating the distance in this way. In other words, we need to know which edge matches with which. To fully perform a shape recognition task we should solve the correspondence problem. However, the aim of the work reported here was to analyze the properties of our length ratio measure and not to solve the full recognition problem. Thus for the experiments reported here we have located the edge correspondences by hand.

For each morphing sequence, in figure 7 we plot the distance between each frame in the sequence and the start and end frames. The monotonicity of the distance is evident throughout the sequences. This is a proof of capacity of our length ratio measure to disambiguate between shapes with topologically similar skeletons.

To further assess the ability to discriminate between similar shapes, we selected a set of topologically similar shapes from a database of images of tools. In the first column of figure 8 we show the selected shapes. To their right are



(a) Distances in fish morphing sequence



(b) Distances in donkey to hare morphing sequence

Fig. 7. Distances from first and last frame of the morphing sequences

the remaining shapes sorted by increasing normalized distance. Each shape is annotated by the value of the normalized distance.

It is clear that similar shapes are usually closest to one-another. However, there are problems due to a high sensitivity to occlusion. This can be seen in the high relative importance given to the articulation angle. This is due to the fact that, in the pliers images, articulation occludes part of nose of pliers. While sensitivity to occlusion is, without a doubt, a drawback of the measure, we have to take into account that skeletal representation in general are highly sensitive to occlusion.

## 6 Conclusions

In this paper we presented a shape measure defined on the skeleton. This measure has been used in the literature as a branch relevance measure during skeleton extraction and pruning. We state that the informational content of the measure goes beyond this use, and can be used to augment the purely structural information residing in a skeleton in order to perform shape indexation and matching tasks.

We show that the shape measure has a number of interesting properties that allow it to distinguish between structurally similar shapes. In particular, the measure a) changes smoothly through topological transitions of the skeleton, b) is able to distinguish between ligature and non-ligature points and to weight them accordingly, and c) it exhibits invariance under "bending". What makes the use of this measure particularly appealing is the fact that it can be calculated with no added effort when the skeleton is computed using the Hamilton-Jacobi method of Siddiqi, Tannenbaum and Zucker.

## References

- [1] C. Arcelli and G. Sanniti di Baja. A width-independent fast thinning algorithm. *IEEE Trans. on PAMI*, 7(4):463-474, 1985.
- [2] J. August, K. Siddiqi, and S. W. Zucker. Ligature instabilities in the perceptual organization of shape. *Comp. Vision and Image Und.*, 76(3):231-243, 1999.
- [3] J. August, A. Tannenbaum, and S. W. Zucker. On the evolution of the skeleton. In *ICCV*, pages 315-322, 1999.
- [4] H. Blum. Biological shape and visual science (part I). *Journal of theoretical Biology*, 38:205-287, 1973.
- [5] G. Borgefors, G. Ramella, and G. Sanniti di Baja. Multi-scale skeletons via permanence ranking. In *Advances in Visual Form Analysis*, 31-42, 1997.


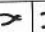

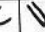

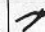



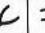
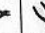
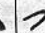













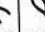




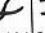

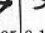
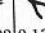



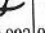
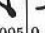
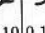
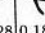


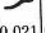


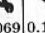
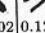
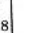
						
	0.068	0.081	0.108	0.112	0.132	0.187
						
	0.053	0.054	0.069	0.080	0.087	0.112
						
	0.030	0.048	0.054	0.084	0.092	0.108
						
	0.021	0.030	0.054	0.081	0.086	0.110
						
	0.080	0.084	0.086	0.095	0.102	0.132
						
	0.088	0.092	0.095	0.110	0.128	0.186
						
	0.021	0.048	0.068	0.069	0.102	0.128

Fig. 8. Some tools and the normalized distance between them

- [6] S. Bouix and Kaleem Siddiqi. Divergence-based medial surfaces. In *Computer Vision ECCV 2000*, 603-618. Springer, 2000. LNCS 1842.
- [7] P. J. Giblin and B. B. Kimia. On the local form and transitions of symmetry sets, medial axes, and shocks. In *ICCV*, 385-391, 1999.
- [8] B. B. Kimia and K. Siddiqi. Geometric heat equation and nonlinear diffusion of shapes and images. *Comp. Vision and Image Understanding*, 64(3):305-322, 1996.
- [9] B. B. Kimia, A. R. Tannenbaum, and S. W. Zucker. Shapes, shocks, and deformations I. *International Journal of Computer Vision*, 15:189-224, 1995.
- [10] P. Klein et al. A tree-edit-distance algorithm for comparing simple, closed shapes. In *ACM-SIAM Symp. on Disc. e Alg.*, 1999.
- [11] R. L. Ogniewicz. A multiscale mat from voronoi diagrams: the skeleton-space and its application to shape description and decomposition. In *Aspects of Visual Form Processing*, 430-439, 1994.
- [12] R. L. Ogniewicz and O. Kübler. Hierarchic voronoi skeletons. *Pattern Recognition*, 28(3):343-359, 1995.
- [13] S. J. Osher and J. A. Sethian. Fronts propagating with curvature dependent speed: Algorithms based on hamilton-jacobi formulations. *J. of Comp. Physics*, 79:12-49, 1988.
- [14] M. Pelillo, K. Siddiqi, and S. W. Zucker. Matching hierarchical structures using association graphs. *PAMI*, 21(11):1105-1120, 1999.
- [15] D. Sharvit, J. Chan, H. Tek, and B. B. Kimia. Symmetry-based indexing of image database. *J. of Visual Comm. and Image Rep.*, 9(4):366-380, 1998.
- [16] A. Shokoufandeh, S. J. Dickinson, K. Siddiqi, and S. W. Zucker. Indexing using a spectral encoding of topological structure. In *CVPR*, 1999.
- [17] K. Siddiqi, S. Bouix, A. Tannenbaum, and S. W. Zucker. The hamilton-jacobi skeleton. In *ICCV*, 828-834, 1999.
- [18] K. Siddiqi and B. B. Kimia. A shock grammar for recognition. In *CVPR*, 507-513, 1996.
- [19] K. Siddiqi, A. Shokoufandeh, S. J. Dickinson, and S. W. Zucker. Shock graphs and shape matching. *International Journal of Computer Vision*, 35(1):13-32, 1999.
- [20] S. Tirthapura et al. Indexing based on edit-distance matching of shape graphs. In *SPIE Int. Symp. on Voice, Video, and Data Comm.*, 25-36, 1998.